

T.D. Sallal , A.M. Abbas\* 

Collage of education for pure sciences (Ibn Al-haitham), University of Baghdad, Baghdad, Iraq

\*e-mail: ahmed.m.a@ihcoedu.uobaghdad.edu.iq

(Received 15 April 2025; received in revised form 14 May 2025; accepted 22 May 2025)

## Preparation and Characterization of Nano-Iron Oxide by using Iraqi Orange Plant Extract and Testing for Adsorption Efficiency

**Abstract:** Nanomaterials, including nanoparticles such as iron oxide nanoparticles, have received great attention from researchers due to their unique properties and applications. There are several diverse methods, including chemical, physical, and green biological methods, to prepare iron oxide nanoparticles. The green method was chosen because it is safer, purer, and less toxic compared to other methods. Therefore, the green method is a promising and environmentally friendly method in the near future. The aqueous extract of Iraqi orange leaves was used to prepare nano iron oxide, it was examined structurally and spectrally by several techniques (X-ray diffraction- XRD, Fourier transform infrared – FT-IR, field emission scanning electron microscopy – FESEM, energy disperse X-ray spectroscopy – EDX, and UV-vis spectroscopy). Through the diagnosis, it was proven that the nano iron oxide was successfully prepared in a spherical form with an average size equal to 68.5 nm. The nano iron oxide particles were tested to remove the crystal dye from its aqueous solution, where the removal percentage reached 61% at 298K, dose adsorbent = 0.01 g, contact time = 90 min, and initial concentration = 11 mg/L. This indicates the possibility of using nano iron oxide which preparing by green method in the field of water treatment.

**Key words:** Fe<sub>3</sub>O<sub>4</sub> NPs, green method, orange leaf aqueous extract, adsorption, crystal violet dye.

### Introduction

Nanotechnology and nanoscience are among the most important modern discoveries because they are the foundation of various areas of modern life. Therefore, they can be described as those materials that are manufactured at a scale of 1-100 nanometers. This size results in dramatic changes in a number of physical and chemical properties of the material. There are several methods for preparing nanomaterials, including chemical reduction, electro-optical deposition, co-deposition, spray thermal decomposition, hydrothermal, and sol-gel [1, 2].

Recently, researchers have focused on conducting an extensive study on the use of magnetic nanoparticles ( $\alpha$ -Fe<sub>2</sub>O<sub>3</sub>,  $\gamma$ -Fe<sub>2</sub>O<sub>3</sub>, Fe<sub>3</sub>O<sub>4</sub>, and FeO) in various general and biomedical applications [3-5]. Hematite ( $\alpha$ -Fe<sub>2</sub>O<sub>3</sub>) is one of the most stable forms of iron oxide. It also has outstanding properties in corrosion treatment, chemical stability, optics, magnetism, and biodegradability at a low cost, which provides ease and possibility of application in various modern applications. Applications of hematite nanoparticles include gas sensors, storage media, dyes, catalysis,

corrosion treatment, solar energy conversion, and water purification [6-8].

There are various methods for manufacturing iron nanoparticles. Some are chemical by using chemical solvents, which can produce toxic chemicals, making it a dangerous and unsafe method. Other methods are physical, but they are expensive because they require high energy. These reasons make us look for other safe and environmentally friendly methods. This is represented by green methods by using living materials and parts in the preparation process [9]. Several previous studies have addressed the preparation of metal nanoparticles and their oxides using the green method through plant extracts and their parts (leaves and roots) as reducing agents [10-13]. Green synthesis of nanoparticles is highly cost-effective, environmentally friendly, and non-toxic. In this green synthesis route, biomolecules in the plant system can act as capping and reducing agents and increase the reduction rate and stability of nanoparticles [14, 15].

In this research, we have performed a green synthesis process for  $\alpha$ -Fe<sub>2</sub>O<sub>3</sub> nanoparticles using aqueous extract of Iraqi orange tree leaves. The prepared iron oxide nanoparticles were characterized by sev-

eral methods (FT-IR, XRD, FESEM, EDX, and UV-VIS), and the prepared samples were tested to determine their efficiency in removing the violet crystal dye from their aqueous solution.

### Materials and methods

**Materials and Reagents.** Solutions and reagents were prepared according to analytical standards and without further purification. Iron nitrate  $\text{Fe}(\text{NO}_3)_2 \cdot 6\text{H}_2\text{O}$  (Sigma-Aldrich), ammonia hydroxide ( $\text{NH}_4\text{OH}$ ) (Sigma-Aldrich), and distilled water. All solutions were prepared with distilled water. Leaves of the orange plant were collected from the local area of Baghdad city in Iraq. Crystal violet dye (CV)  $\text{C}_{25}\text{N}_3\text{H}_{30}\text{Cl}$  for adsorption tests.

**Preparation of leaves of orange plant extract.** Orange leaves were collected from one of the orchards of the Suleiman Pak area located on the Tigris River in Baghdad Governorate. They were then washed with distilled water several times to get rid of dust and other pollutants. After washing, the leaves were dried at room temperature for seven days without exposing them to sunlight. Bitter orange extract was prepared in water by adding 200 ml of distilled water to 20 grams of dried bitter orange leaf powder in a 500 ml beaker with continuous stirring and heating at a temperature of  $60^\circ\text{C}$  for an hour. Then the mixture was left after heating for 24 hours. The next day, the filtration process was carried out to obtain a clear brown bitter orange extract, which is then stored in special, tightly sealed bottles. and refrigerated for further use.

**Synthesis and characterization of iron oxide nanoparticles.** 10 mL of a 0.01 M solution of iron nitrate with distilled water was placed in a beaker with stirring using a magnetic stirrer (Hot Plate and Magnetic Stirrer, LMS-100, Korea) for 30 min. Then it was continuously stirred in a reducing agent and a covering agent of the prepared orange leaf extract until the mixture turned dark brown and a precipitate formed. To ensure a homogeneous reaction, this process was carried out with continuous stirring. The collected precipitate solution was centrifuged (Hermie Laborti Chink Type Z 200 A, 6000 rpm, Germany) at 5000 rpm for 20 min with DI water repeatedly. The dried precipitate powder was heated at  $700^\circ\text{C}$  for 8 h (Furnaces oven Vindon LTD, Oldham, England) to obtain dark red  $\text{Fe}_3\text{O}_4$  nanoparticles.

The NPs were characterized by using a field emission scanning electron microscope (FESEM, ZEISS model: Sigma VP-UK). X-ray diffraction (XRD) patterns were obtained using Siemens model

D500, Germany. Surface functional groups of the NPs were determined by using Fourier-transform infrared spectroscopy (FTIR, IRPrestige-21 Shimadzu, Japan). The optical transmission/absorption spectra of the particles in deionized water were recorded using a UV-VIS spectrometer (Shimadzu 1800, Japan) and energy disperse x-ray spectroscopy (EDX, Oxford Instruments, UK).

**Adsorption experiments.** The adsorption experiment was conducted by applying a continuous system by taking a weight (0.01 g) of the  $\text{Fe}_3\text{O}_4$  NPs and bringing it into contact with the volume (10 ml) of (CV) dye solution at a concentration of 11 mg/L by using a water bath shaker (Labtech, South Korea) at laboratory temperature, 150 rpm agitation speed, and over time periods 0–120 min, and each sample is separated by a centrifuge in order to be measured. Each solution was analyzed by the spectrometer (Shimadzu 1800, Japan), and the amount of adsorbed dye and the percentage of adsorption (A%) are calculated through the following equations (1, 2), respectively [16, 17]:

$$q_e = \left( \frac{C_o - C_t}{m} \right) V \quad (1)$$

$$\%A = \left( \frac{C_o - C_t}{C_o} \right) \times 100 \quad (2)$$

where  $C_o$  and  $C_t$  are the CV dye concentrations at time ( $t = \text{zero}, t$ ) respectively. The  $V(\text{L})$  represents the volume of the CV dye solution, whereas  $m(\text{g})$  symbolizes the adsorbent weight [18, 19].

### Results and discussion

#### Characterization of $\text{Fe}_3\text{O}_4$ NPs

**XRD analysis.** Figure 1 shows the XRD pattern of the intermediate iron oxide nanoparticles in orange leaf water extract within the range ( $2\theta = 5-80^\circ$ ) showed weak and few peaks, reflecting the low level of crystallinity in the resulting material. In addition, the diffraction peaks were identified at 31.18, 33.34, 35.79, 40.95, 49.56, 54.27, and 64.14, respectively, indexed to 10-2, 104, 110, 20-4, and 116, which belong to magnetite nanoparticles  $\text{Fe}_3\text{O}_4$  (JCPDS 00-019-062). There were no additional peaks in the XRD pattern, indicating the high purity of the  $\alpha\text{-Fe}_2\text{O}_3$  nanoparticles. The average crystallite size calculated using the Debye-Scherrer equation for the synthesized green hematite nanoparticles was about 68.5 nm [20, 21].

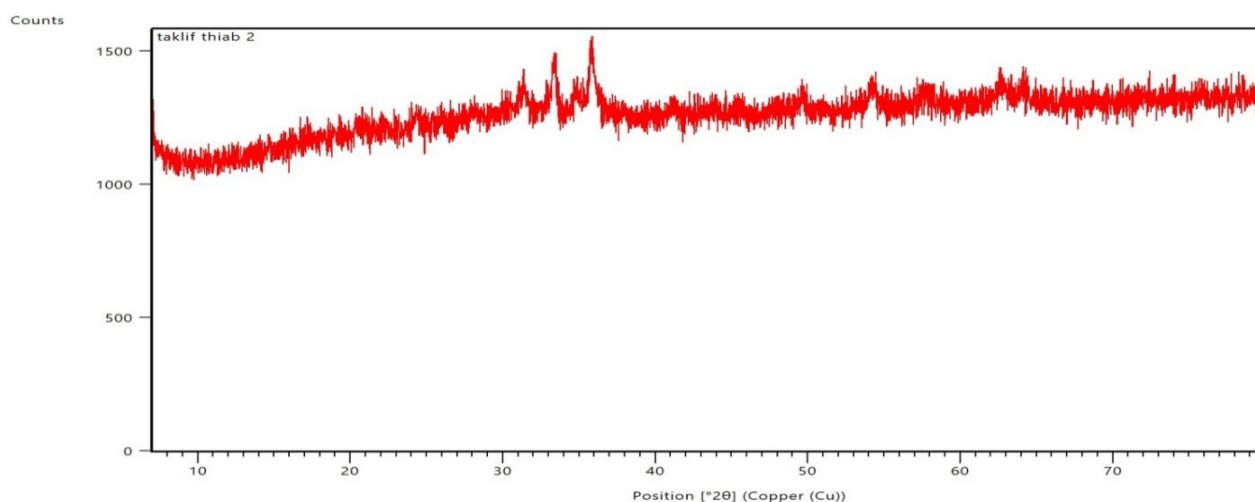


**Figure 1** – XRD pattern of iron oxide ( $\alpha\text{-Fe}_2\text{O}_3$ )

*FT-IR analysis.* Figure 2 FTIR analysis shows the functional groups of phytochemicals and  $\text{Fe}_3\text{O}_4$  nanoparticles within the range  $400\text{-}4000\text{ cm}^{-1}$ . Weak peaks were found at  $3087$  and  $2885\text{ cm}^{-1}$  due to the stretching of the aromatic and aliphatic C-H groups, respectively. There is also a peak at  $1510\text{ cm}^{-1}$  attributed to the stretching of the N=O group, while the peak  $1112\text{ cm}^{-1}$  is attributed to the stretching

of C-O. Therefore, all peaks can be attributed to the phytochemicals in the aqueous extract, which are supposed to be responsible for the reduction of metal ions and their forms to the nanomaterials. The presence of magnetite nanoparticles can also be confirmed by the strong peaks around  $455$  and  $534\text{ cm}^{-1}$  corresponding to the Fe-O stretches of  $\text{Fe}_3\text{O}_4$  [22, 23].

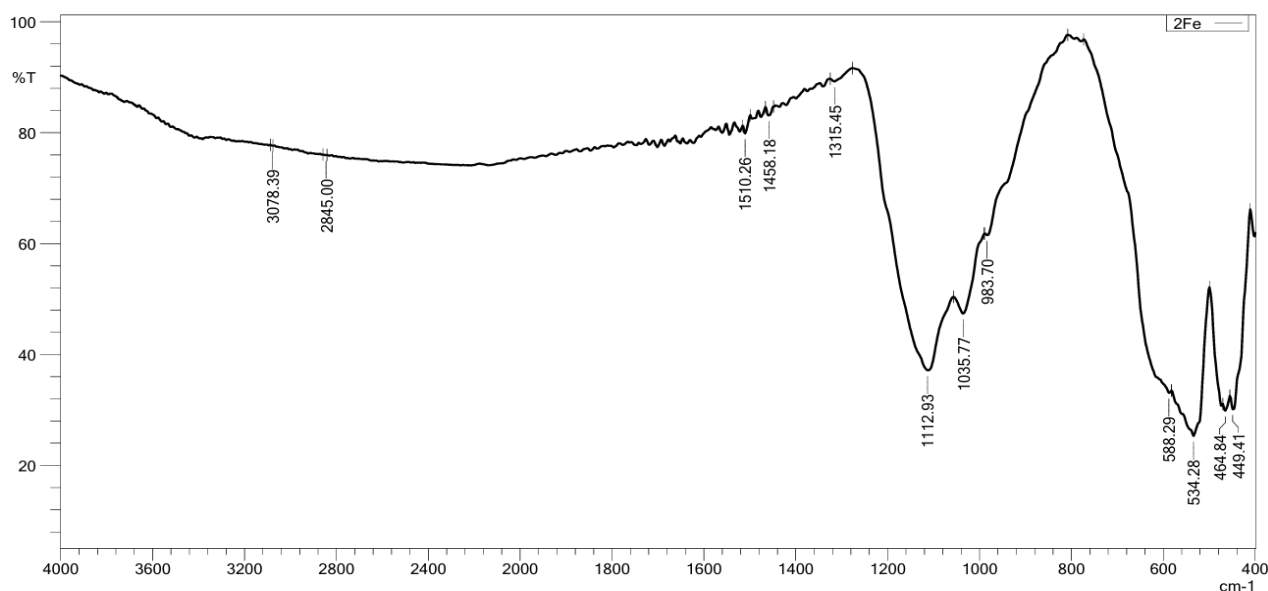


**Figure 2** – Spectrum FT-IR pattern of iron oxide NPs

*FE-SEM analysis.* Figure 3 shows a field-emitted scanning electron microscope image of the surface morphology of the synthesized iron oxide nanoparticles in the orange leaf aquatic extract at a magnification level of 100 nm. The image showed the aggregation

of particles in the form of extended, heterogeneous, semi-spherical nano-clusters of  $\text{Fe}_3\text{O}_4$ . The size of these particles reaches 30 nm in that specific part of the image, and it agrees with the average size calculated according to XRD data in being less than 100 nm [24].

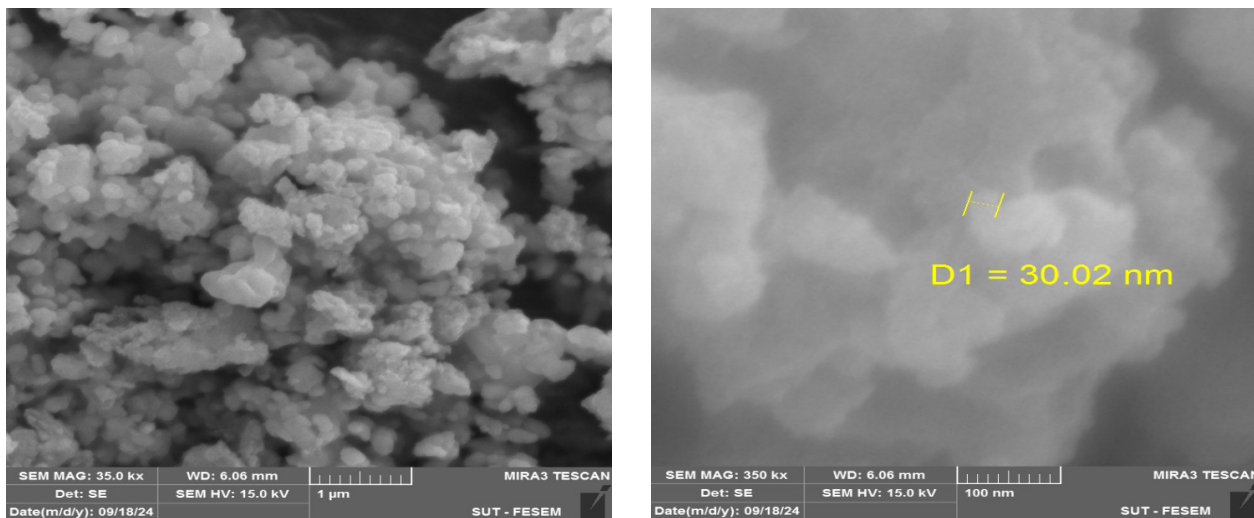


**Figure 3** – SEM observation of iron oxide NPs at 100nm,1  $\mu\text{m}$

*EDX Analysis.* Figure 4 shows the energy dispersion X-ray (EDX) results of  $\text{Fe}_3\text{O}_4$  nanoparticles that were manufactured in a green and environmentally friendly way (orange leaf aquatic extract). The per-

centages of the elements that make up the resulting nano-iron oxide were as follows: 80.04% of O and 19.96% of Fe, indicating the success of preparing nano-iron oxide with high purity [25, 26].

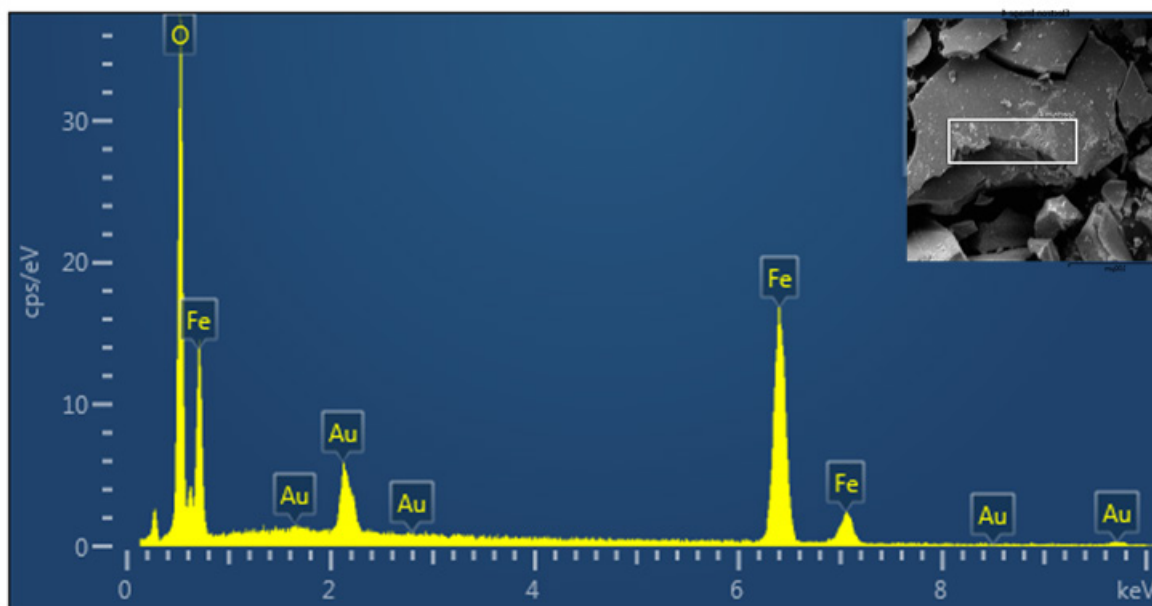


**Figure 4** – EDX Analysis of iron oxide NPs

*UV-vis analysis.* Figure 5 shows the UV-vis spectrum in the range 300-600 nm and here reflects the characteristic formation of nanoparticles during

color change based on absorption spectra. The characteristic peak at 318 nm confirmed the formation of  $\text{Fe}_3\text{O}_4$  nanoparticles [23].

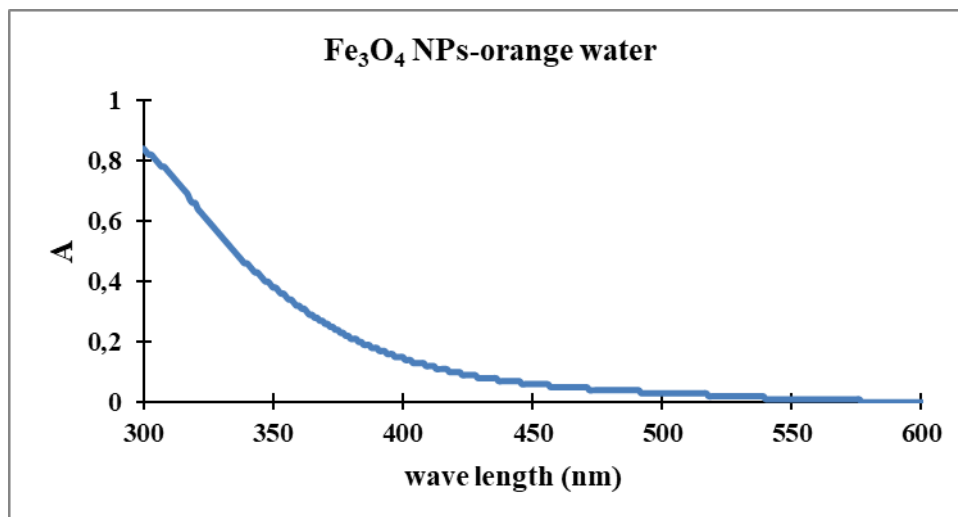


Figure 5 – UV-Vis spectrum of iron oxide NPs

*Study of CV dye adsorption.* The adsorption efficiency of iron nanoparticles CV dye was studied over a time period of 15-180 min and at constant conditions including pH 7, initial CV concentration of 11 mg/L,  $\text{Fe}_3\text{O}_4$  nanoparticle weight of 0.01 g, and vibration speed of 150 rpm at 298 K. The amount of adsorbed CV dye increases with time and reaches

equilibrium at about 90 min, after which the removal rate remains constant. This may indicate that CV particles with a large surface area can adhere to the  $\text{Fe}_3\text{O}_4$  nanoparticle adsorbent for at least 90 min after saturation of the unoccupied surface sites, with adsorption efficiency up to 61% ( $q_c = 6.7$  mg/g) as shown in Figures 6 and 7 [27, 28].

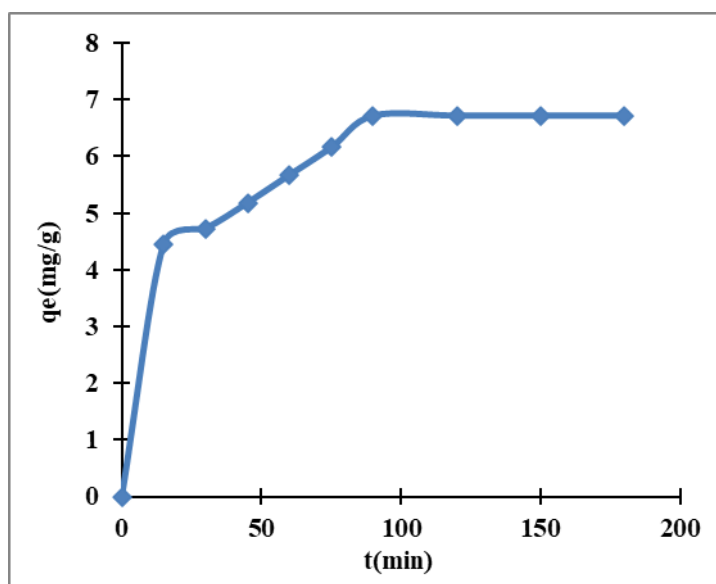


Figure 6 – Effect of contacting time on the quantity adsorption of CV dye on  $\text{Fe}_3\text{O}_4$  NPs

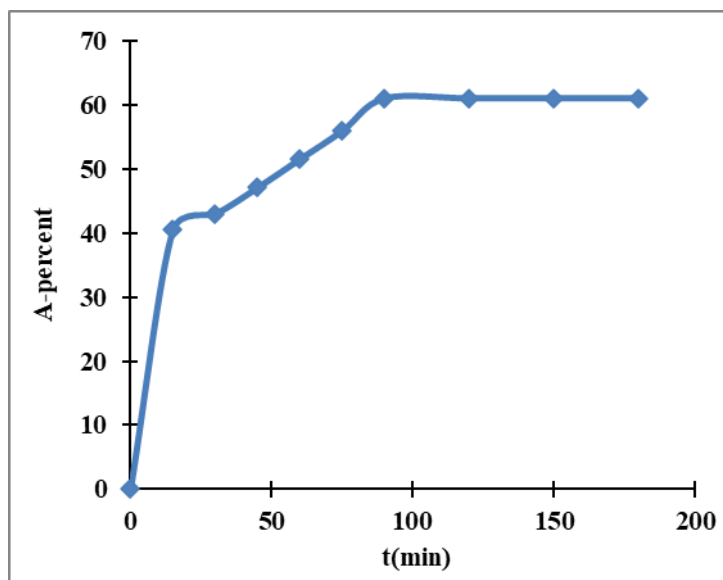


Figure 7 – Effect of contacting time on the percent adsorption of CV dye on  $\text{Fe}_3\text{O}_4$  NPs

## Conclusion

This study concludes the success of applying the green method by using the aqueous extract of orange leaves with reduction and coating in the preparation of nano-ferric oxide particles. This was confirmed by using several techniques. Through the X-ray diffraction technique (XRD) and the Debye-Scherrer equation and matching it with standard data, we conclude that they are low-crystalline nanomaterials with an average size of 68.5 nm. From the Fourier transform infrared technique (FT-IR), the presence of the active group Fe-O which is due to the nano-iron oxide, while we concluded the semi-spherical shape from the images of the scanning electron microscope with the emission field (FESEM). By measuring the disperse energy of the X-ray spectroscopy (EDX) and the ratio of iron to oxygen, we found that the prepared materials are iron oxide with high purity. From measuring the UV-vis spectroscopy, there is a broad

peak starting from wave length 400 nm and extending to 300 nm, which indicates that the prepared material is nano-iron oxide. The nano-iron oxide was tested in the field of treating water pollution with organic dyes, which is the crystal violet dye (CV), and showed good efficiency in removing the CV dye. The purple crystalline color gives a good impression of the efficiency of green materials in water treatment.

## Acknowledgments

The authors thank the Department of Chemistry, College of Education for Pure Sciences, Ibn Al-Haytham, University of Baghdad for their assistance with tools, equipment, and laboratories.

## Conflict of interest

The authors declare the absence a conflict of interest warranting disclosure in this article.

## References

1. Veeranna S., Burhanuddin A., Khanum S., Narayan S. L., Pratima K. (2013) Biosynthesis and antibacterial activity of silver nanoparticles. *Res. J. Biotechnol.*, 8, pp. 11-17. [https://www.researchgate.net/publication/287478569\\_Biosynthesis\\_and\\_antibacterial\\_activity\\_of\\_silver\\_nanoparticles](https://www.researchgate.net/publication/287478569_Biosynthesis_and_antibacterial_activity_of_silver_nanoparticles)
2. Lassoued A., Dkhil B., Gadri A., Ammar S. (2017) Control of the shape and size of iron oxide ( $\alpha\text{-Fe}_2\text{O}_3$ ) nanoparticles synthesized through the chemical precipitation method. *Results Phys.*, 7, pp. 3007-3015. <https://doi.org/10.1016/j.rinp.2017.07.066>.
3. Ali A., Zafar H., Zia M., ul Haq I., Phull A.R., Ali J.S., Hussain A. (2016) Synthesis, characterization, applications, and challenges of iron oxide nanoparticles. *Nanotechnol Sci Appl.*, 9, pp. 49-67. <https://doi.org/10.2147/NSA.S99986>.

4. Wu W., He Q., Jiang C. (2008) Magnetic iron oxide nanoparticles: synthesis and surface functionalization strategies. *Nanoscale Res. Lett.*, 3, pp. 397-415. <https://doi.org/10.1007/s11671-008-9174-9>.
5. Teja A.S., Koh P.Y. (2009) Synthesis, properties, and applications of magnetic iron oxide nanoparticles. *Prog. Cryst. Growth Charact. Mater.*, 55, pp. 22-45. <https://doi.org/10.1016/j.pcrysgrow.2008.08.003>.
6. Kefeni K.K., Msagati T. A., Nkambule T.T., Mamba B.B. (2018) Synthesis and application of hematite nanoparticles for acid mine drainage treatment. *J. Environ. Chem. Eng.*, 6, pp. 1865-1874. <https://doi.org/10.1016/j.jece.2018.02.037>.
7. Wu C., Yin P., Zhu X., OuYang C., Xie Y. (2006) Synthesis of hematite ( $\alpha$ -Fe<sub>2</sub>O<sub>3</sub>) nanorods: diameter-size and shape effects on their applications in magnetism, lithium ion battery, and gas sensors. *J. Phys. Chem. B*, 110, pp. 17806-17812. <https://doi.org/10.1021/jp0633906>.
8. Alshehri A., Malik M. A., Khan Z., Al-Thabaiti S.A., Hasan N. (2017) Biofabrication of Fe nanoparticles in aqueous extract of Hibiscus sabdariffa with enhanced photocatalytic activities. *RSC Adv.*, 7, pp. 25149-25159. <https://doi.org/10.1039/C7RA01251A>.
9. Ruddaraju L.K., Pammi S.V.N., sankar Guntuku G., Padavala V.S., Kolapalli V.R.M. (2020) A review on anti-bacterials to combat resistance: From ancient era of plants and metals to present and future perspectives of green nano technological combinations. *Asian J. Pharm. Sci.*, 15, pp. 42-59. <https://doi.org/10.1016/j.ajps.2019.03.002>.
10. Pallela P.N.V.K., Ummey S., Ruddaraju L.K., Pammi S.V.N., Yoon S.G. (2018) Ultra Small, mono dispersed green synthesized silver nanoparticles using aqueous extract of *Sida cordifolia* plant and investigation of antibacterial activity. *Microb. Pathog.*, 124, pp. 63-69. <https://doi.org/10.1016/j.micpath.2018.08.026>.
11. Acharyulu N.P.S., Madhu Kiran P., Pratap K., Kalyani R.L., Pammi S.V.N. (2014) Room temperature synthesis and evaluation of antibacterial activity of silver nanoparticles using *Phyllanthus amarus* leaf extract. *J. Bionanoscience*, 8, pp. 190-194. <https://doi.org/10.1166/jbns.2014.1220>.
12. Radhi I.M., Abd S.S., Faraj R.A.S., Abbas A.M., Himdan T.A. (2024) Using activated and modified adsorbent surfaces from banana peels to remove the green Janus dye: A Kinetic, Isothermal, and Thermodynamic Study. *Mong. J. Chem.*, 25, pp. 1-15. <https://doi.org/10.5564/mjc.v25i52.3450>.
13. Pallela P.N.V.K., Ummey S., Ruddaraju L.K., Kollu P., Khan S., Pammi S.V.N. (2019) Antibacterial activity assessment and characterization of green synthesized CuO nano rods using *Asparagus racemosus* roots extract. *SN Appl. Sci.*, 1, pp. 1-7. <https://doi.org/10.1007/s42452-019-0449-9>.
14. Pallela P.N.V.K., Ummey S., Ruddaraju L.K., Gadi S., Cherukuri C.S.L., Barla S., Pammi S.V.N. (2019) Antibacterial efficacy of green synthesized  $\alpha$ -Fe<sub>2</sub>O<sub>3</sub> nanoparticles using *Sida cordifolia* plant extract. *Heliyon*, 5, pp. e02765. <https://doi.org/10.1016/j.heliyon.2019.e02765>.
15. Hemalatha S., Venkatesan R.S. (2021) Fabrication of Iron Oxide Nano Particle Using Cassia Auriculata leaf Extract and its Characterization. *Ann Rom Soc Cell Biol*, 25, pp. 1683-1689. <http://annalsofrscb.ro/index.php/journal/article/view/1614>.
16. Jasim M.A., Abbas A.M., Radhi I.M. (2021) Preparation and characterization of biomass-alumina composite as adsorbent for safranin-o dye from aqueous solution at different temperatures. *AIP Conf. Proc.*, 2372, pp. 120001-120012. <https://doi.org/10.1063/5.0068746>.
17. Abbas A.M., Abd S.S., Abdulhadi H.T. (2018) Kinetic Study of Methyl Green Dye Adsorption from Aqueous Solution by Bauxite Clay at Different Temperatures. *Ibn al-Haitham J. Pure Appl. Sci.*, 31, pp. 58-66. <https://doi.org/10.30526/31.1.1853>.
18. Mizhir A.A., Al-Lami H.S., Abdulwahid A.A. (2022) Kinetic, isotherm, and thermodynamic study of bismarck brown dye adsorption onto graphene oxide and graphene oxide-grafted-poly (n-butyl methacrylate-co-methacrylic acid). *Baghdad Sci. J.*, 19, pp. 0132-0132. <https://doi.org/10.21123/bsj.2022.19.1.0132>.
19. Saed S.A., AL-Mammar D.E. (2021) Influence of Acid Activation of a Mixture of Illite, Koalinite, and Chlorite Clays on the Adsorption of Methyl Violet 6B Dye. *Iraqi J. Sci.*, 62(6), pp. 1761-1778. <https://doi.org/10.24996/ijcs.2021.62.6.2>.
20. Rasha T.S., Dunya E.A. (2023) Adsorption of Azo Dye Onto TiO<sub>2</sub> Nanoparticles Prepared by a Novel Green Method: Isotherm and Thermodynamic Study. *Iraqi J. Sci.*, 64(8), pp. 3779-3792. <https://doi.org/10.24996/ijcs.2023.64.8.5>.
21. Abbas A.M., Mohammed Y.I., Himdan T.A. (2017) Adsorption kinetic and thermodynamic study of congo red dye on synthetic zeolite and modified synthetic zeolite. *Ibn al-Haitham J. Pure Appl. Sci.*, 28, pp. 54-72. <https://jih.uobaghdad.edu.iq/index.php/j/article/view/190>.
22. Abbas A.M., Abdulrazzak F.H., Radhi I.M., Himdan T.A., Hussein F.H. (2020) Purification Techniques for Cheap Multi-Walled Carbon Nanotubes. *J. Phys. Conf. Ser.*, 1660, pp. 012022. <https://doi.org/10.1088/1742-6596/1660/1/012022>.
23. Rufus A., Sreeju N., Philip D. (2016) Synthesis of biogenic hematite ( $\alpha$ -Fe<sub>2</sub>O<sub>3</sub>) nanoparticles for antibacterial and nanofluid applications. *RSC Adv.*, 6, 94206-94217. <https://doi.org/10.1039/C6RA20240C>.
24. Jawad H., Abbas A.M. (2021) Study of Efficacy Adsorption of Methyl Green by Attapulgite and Modified Attapulgite Clay from Aqueous Solution. *Ibn al-Haitham J. Pure Appl. Sci.*, 34, pp. 19-29. <https://doi.org/10.30526/34.1.2550>.
25. Kazem M.S., Abbas A.M. (2022) Study of inorganic doping of kaolin clay, a kinetic study of adsorption of methyl green dye from its aqueous solutions. *Eurasian Chem. Commun.*, 4(12), pp. 1218-1227. <https://doi.org/10.22034/ecc.2022.342243.1467>
26. Abbas A.M., Merza S.H. (2020) Preparation and Characterization of Graphene Oxide-Attapulgite composite and its use in kinetic study of Alizarin Dye Adsorption from Aqueous Media. *Egypt. J. Chem.*, 63, pp. 561-572. <https://doi.org/10.21608/ejchem.2019.15600.1946>.

27. Yass D.A., Abbas A.M. (2024) Study the efficiency of titanium dioxide nanoparticles for water treatment from Congo red dye. *Her. Bauman Mosc. State Tech. Univ. Ser. Nat. Sci.*, 115, pp. 121–131. <https://vestniken.bmstu.ru/eng/catalog/chem/orch/1163.html>.
28. Faraj R.A.S., Abbas A.M. (2021) Loading and Activating a Carbon Surface and Applied for Congo Red Adsorption, Kinetic Study. *J. Phys. Conf. Ser.*, 1879, pp. 022076. <https://doi.org/10.1088/1742-6596/1879/2/02207>.

**Information about authors**

*Takleef Dheyab Sallal – Assistant Lecturer, Collage of education for pure sciences (Ibn Al-haitham), University of Baghdad (Baghdad, Iraq, e-mail: sallaltakleef535@gmail.com)*

*Ahmed Mohammed Abbas – PhD, Assistant Professor, Collage of education for pure sciences (Ibn Al-haitham), University of Baghdad (Baghdad, Iraq, e-mail: ahmed.m.a@ihcoedu.uobaghdad.edu.iq)*